

Signature of elasticity in the Faraday instability

Pierre Ballesta* and Sébastien Manneville

Centre de Recherche Paul Pascal, Avenue Schweitzer, 33600 Pessac, FRANCE

(Dated: February 2, 2008)

We investigate the onset of the Faraday instability in a vertically vibrated wormlike micelle solution. In this strongly viscoelastic fluid, the critical acceleration and wavenumber are shown to present oscillations as a function of driving frequency and fluid height. This effect, unseen neither in simple fluids nor in previous experiments on polymeric fluids, is interpreted in terms of standing elastic waves between the disturbed surface and the container bottom. It is shown that the model of S. Kumar [Phys. Rev. E, **65**, 026305 (2002)] for a viscoelastic fluid accounts qualitatively for our experimental observations. Explanations for quantitative discrepancies are proposed, such as the influence of the nonlinear rheological behaviour of this complex fluid.

PACS numbers: 47.50.+d, 47.20.-k, 83.60.-a, 47.54.+r

Since Faraday's founding work [1], the parametric instability of a vertically vibrated fluid layer has emerged as one of the best candidates to study pattern formation and nonlinear dynamics. Above a critical acceleration a_c , an initially flat and quiescent fluid layer driven vertically at frequency f goes unstable and gives way to a pattern of surface waves that oscillates at half the driving frequency with a characteristic wavenumber k_c [1, 2, 3]. As the driving acceleration is raised above onset, a series of secondary instabilities take place, leading to defect dynamics and eventually to spatio-temporal chaos [4].

So far, the Faraday instability has been mostly studied in *simple* viscous fluids [1, 2, 3, 4, 5, 6]. Recently, interest has grown in the effect of vertical vibrations on a layer of *complex* fluid, both experimentally [7, 8] and theoretically [9, 10]. Due to their microstructure, complex fluids display viscoelastic properties, which may affect classical hydrodynamic instabilities [11]. However, previous experiments on semidilute polymeric solutions did not show significant modifications of the Faraday instability [7, 8]. The debate has mainly focused on the existence of a harmonic response (at f) instead of the classical subharmonic response (at $f/2$), a typical viscoelastic effect predicted numerically [9, 10] and observed experimentally at rather low frequencies ($f < 40$ Hz) together with new types of patterns that compete with each other [8].

In this Letter, we report onset measurements of the Faraday instability in a wormlike micelle solution, a strongly viscoelastic fluid well characterized by a single relaxation time τ . The critical acceleration and wavenumber are shown to present *oscillations* as a function of driving frequency (see Fig. 1). This effect is interpreted in terms of standing elastic waves between the disturbed surface and the container bottom. It is also shown that the finite-depth model of Ref. [9] accounts qualitatively for these experimental observations. Finally, possi-

ble explanations for discrepancies are discussed and the implications of our results in the field of complex fluid hydrodynamics are emphasized.

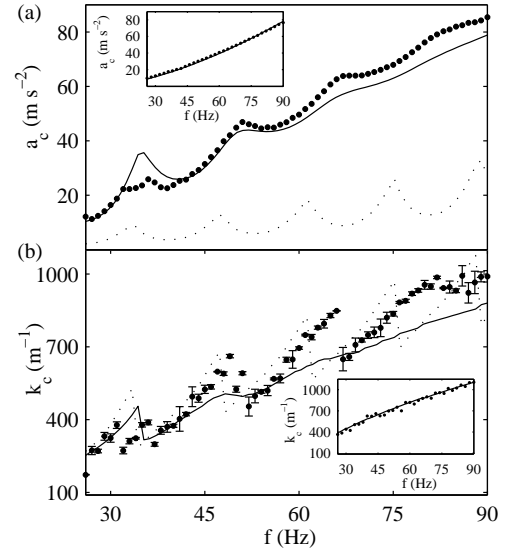


FIG. 1: (a) Critical acceleration a_c and (b) critical wavenumber k_c vs driving frequency in a 4 % wt. CPCl/NaSal wormlike micelle solution (\bullet). Also shown are the calculations for the corresponding Maxwell fluid (dotted lines) and when adding a Zimm-like term (solid lines). Insets: a_c and k_c for a Newtonian fluid (78 % glycerol-22 % water mixture) and corresponding predictions using the model of Ref. [6] with density $\rho = 1.19 \text{ g cm}^{-3}$, viscosity $\eta = 0.05 \text{ Pa s}$, and surface tension $\sigma = 0.06 \text{ N m}^{-1}$ (solid lines).

Wormlike micelles (also called “living polymers”) are long, cylindrical aggregates of surfactant molecules in solution [11]. They spontaneously form under given conditions of temperature and concentration for a wide range of surfactants. Unlike conventional polymers, their size is not fixed and they constantly break and recombine under thermal agitation. Their dynamics thus result from both a classical reptation motion [12] and break-

*Corresponding author: ballesta@crpp-bordeaux.cnrs.fr

ing/recombination processes [13]. This peculiar feature leads to an almost perfect Maxwellian behaviour in the small-deformation regime, for which the complex viscosity reads: $\eta_M(\omega) = G_0\tau/(1+i\omega\tau)$, where G_0 is the shear modulus, τ the relaxation time, and ω the pulsation.

Our working fluid is a wormlike micelle system made of cetylpyridinium chloride (CPCl, from Aldrich) and sodium salicylate (NaSal, from Acros Organics) dissolved in brine (0.5 M NaCl) [14, 15]. In this study, we focus on a 4 % wt. sample with a concentration ratio $[\text{NaSal}]/[\text{CPCl}] = 0.5$ as described in Ref. [15]. Linear rheological measurements were performed in the cone-and-plate geometry using a stress-controlled rheometer (AR 2000N, TA Instruments) with small stress oscillations of amplitude 2 Pa (the linear regime extends up to 20 Pa). As shown in Fig. 2, the dynamic moduli are well accounted for by a Maxwell model $G'(\omega) = -\omega\Im(\eta_M(\omega))$ and $G''(\omega) = \omega\eta_s + \omega\Re(\eta_M(\omega))$, with $G_0 = 16$ Pa and $\tau = 0.44$ s, at least for frequencies below 2 Hz. $\eta_s = 10^{-3}$ Pa s represents the solvent (brine) contribution to the viscosity.

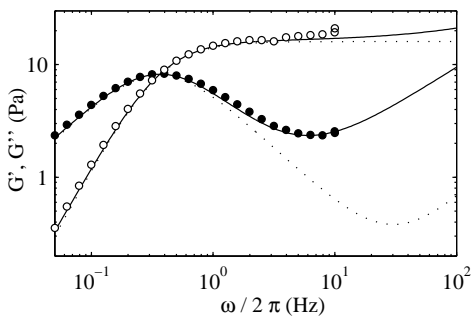


FIG. 2: Storage modulus $G'(\omega)$ (○) and loss modulus $G''(\omega)$ (●) as a function of oscillation frequency $\omega/2\pi$ for a stress amplitude of 2 Pa. The dotted line is the best Maxwell fit ($G_0 = 16$ Pa and $\tau = 0.44$ s) with a solvent viscosity $\eta_s = 10^{-3}$ Pa s. The solid line corresponds to the same Maxwell model with an added Zimm-like term (see text).

Our experimental setup is a classical one for studying the Faraday instability. A cylindrical container of inner diameter 60 mm is filled to a height $h = 10$ mm under the brimful boundary condition [5] and vertically vibrated using an electromagnetic shaker (Ling Dynamic Systems V406). The fluid temperature is regulated to $21 \pm 0.05^\circ\text{C}$ by water circulation beneath the container. In order to prevent evaporation and surface contamination, the container is sealed by a Plexiglas cover that supports a small piezoelectric accelerometer (Endevco 2224C). The signal from the accelerometer is fed to a lock-in amplifier (Stanford Research Systems SR810) that provides the sinusoidal excitation at frequency f to the shaker. The experiment is illuminated from above by a circle of diodes strobed at f or $f/2$. The bottom of the container is made of aluminum to provide mechanical rigidity, and anodized

to prevent light reflection.

For a given driving frequency, the instability threshold is determined by (i) noting the acceleration for which the instability first appears, (ii) fully destabilizing the whole surface by increasing the acceleration about 5 % above onset, and (iii) decreasing the acceleration and noting the acceleration for which the instability completely disappears. In all cases, the two values of the critical acceleration differ by less than 2 %: no significant hysteresis is observed. The value of a_c shown in Fig. 1(a) is the mean of these two accelerations, their difference remaining always smaller than the marker size. Moreover, the surface response was found to be *subharmonic* (at $f/2$) over the whole range of investigated frequencies $f = 25$ –90 Hz. For each frequency, the critical wavenumber k_c is estimated from a picture of the fully destabilized surface.

Figure 1 constitutes our main result. The critical acceleration and wavenumber are not monotonic but rather oscillate with the frequency, a maximum in a_c corresponding to a large drop of k_c . To our knowledge, such a marked effect has not been reported in previous experiments on complex fluids. In Newtonian fluids, non-monotonic a_c or k_c are associated to *lateral* boundary effects (as only an integer or semi-integer number of wavelengths may fit in the cell when the brimful condition is used) [5, 16]. In order to rule out such an interpretation, we repeated the experiment with a Newtonian fluid of critical acceleration and wavenumber similar to our wormlike micelle solution. The insets in Fig. 1 show monotonic behaviours, in perfect agreement with the model of Ref. [6] for a laterally unbounded viscous fluid, as already found in other Newtonian fluids [5]. This allows us to consider our results in terms of a laterally unbounded fluid and confirms the viscoelastic nature of the oscillations seen in a_c and k_c for the wormlike micelles.

More precisely, we propose to interpret these oscillations as a coupling between the disturbed surface and elastic waves reflected at the container bottom. For a Maxwell fluid in the $\omega\tau \gg 1$ limit, which is always verified in our experiments, the velocity c and attenuation coefficient α of shear waves are given by $c = \sqrt{G_0/\rho}$ and $\alpha = 1/(2c\tau)$, where ρ is the fluid density. Above onset, surface disturbances generate elastic waves that may form a standing wave in the container height h . When $2h$ is a semi-integer multiple of the wavelength $2c/f$ [17], i.e. $f = (n + 1/2)f_1$ with $f_1 = \sqrt{G_0/\rho}/h$ and n an integer, constructive interferences form at the surface. In this case, elastic waves are amplified and surface disturbances are promoted so that the critical acceleration is expected to be lower than in the absence of elastic effects. On the other hand, when $f = nf_1$, destructive interferences should lead to an increase of a_c , hence the oscillations of Fig. 1(a). Moreover, at each maximum of a_c , the number of elastic modes in the vertical direction increases. Since the vertical wavenumber is linked to the horizontal one through the incompressibility condition [6, 9], jumps sim-

ilar to those of Fig. 1(b) are expected even in a laterally unbounded fluid.

In order to further check the above interpretation, we performed the finite-depth numerical calculations of Ref. [9] for a Maxwell fluid with the rheological parameters inferred from Fig. 2. The two remaining parameters used in the calculations, namely the density and the surface tension of the fluid, were measured independently yielding $\rho = 1.0 \text{ g cm}^{-3}$ and $\sigma = 0.03 \text{ N m}^{-1}$ respectively. By varying h (G_0 resp.) for a fixed G_0 (h resp.), we show in Fig. 3 that large oscillations also show up numerically. Moreover, they perfectly agree with the simple relation $f_n = n\sqrt{G_0/\rho}/h$ suggested above. The interpretation in terms of elastic waves reflected at the container bottom is thus confirmed. This *finite-depth* viscoelastic effect went unseen in previous numerical studies that focused on the question of harmonic vs subharmonic response [9, 10].

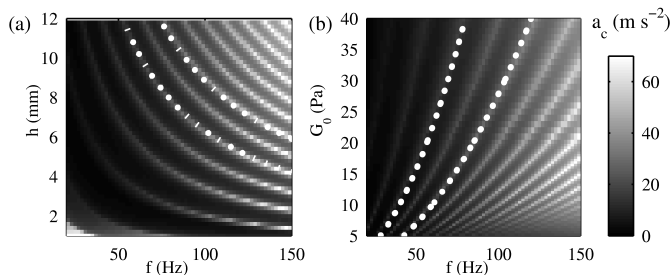


FIG. 3: Numerical calculations using the model of Ref. [9] with $\tau = 0.44 \text{ s}$, $\rho = 1.0 \text{ g cm}^{-3}$, and $\sigma = 0.03 \text{ N m}^{-1}$. (a) a_c vs h and f at fixed $G_0 = 16 \text{ Pa}$. (b) a_c vs G_0 and f at fixed $h = 10 \text{ mm}$. White dots are the lines $f_n = n\sqrt{G_0/\rho}/h$ with $n = 5$ and 7 and coincide with maxima of a_c .

Note, however, that these numerical calculations based on the Maxwell model do not allow any quantitative comparison with the experimental a_c and k_c (see dotted lines in Fig. 1). This is most probably because our fluid does not remain purely Maxwellian at frequencies higher than 2 Hz . Indeed, although our rheological measurements are limited to 10 Hz , an upturn of $G''(\omega)$ is clearly visible on the data of Fig. 2. Such an upturn is usually attributed to the presence of Rouse-like or Zimm-like motion at high frequencies [12, 18]. If we model this behaviour by adding a Zimm relaxation term to the previous Maxwell model,

$$\eta(\omega) = \eta_s + \frac{G_0\tau}{1 + i\omega\tau} + a_Z \left(1 - \frac{i}{\sqrt{3}}\right) \omega^{-\frac{1}{3}}, \quad (1)$$

a very good fit of both $G'(\omega)$ and $G''(\omega)$ is obtained with $a_Z = 0.12 \text{ Pa s}^{2/3}$ (see solid lines in Fig. 2).

Using Eq. (1) in the numerical calculations leads to computed curves (shown as solid lines in Fig. 1) that are much closer to the experimental measurements, although the attenuation of the oscillations with increasing frequency is now too strong (see discussion below).

Finally, both our simple analysis and the numerical results of Fig. 3(a) predict that a_c and k_c should oscillate when the fluid height h is varied at a fixed frequency. Figure 4 shows that such oscillations indeed take place in the experiment and that the Maxwell model corrected by a Zimm-like term provides a good description of a_c . Again, these findings are strikingly different from the monotonic decay of a_c vs h in Newtonian fluids [5].

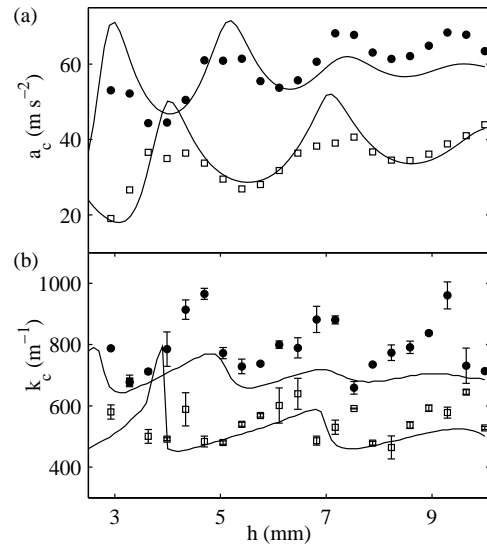


FIG. 4: (a) Critical acceleration a_c and (b) critical wavenumber k_c vs fluid height measured at 50 Hz (\square) and at 70 Hz (\bullet). The solid lines correspond to the Maxwell model with an added Zimm-like term (see text).

Let us now discuss the present experimental and numerical results. Previous experiments on polymeric solutions did not show any oscillations in the onset measurements [7, 8]. This can be explained by considering the attenuation coefficient of the elastic waves α . If $\alpha > 1/h$, no standing wave, and thus no oscillation, is observed due to a too strong attenuation. In our wormlike micelle solution, the storage modulus $G'(\omega)$ remains always at least three times larger than the loss modulus $G''(\omega)$ and $\alpha h \simeq 0.09$, so that oscillations are observed, whereas previous experiments were performed either in the capillary regime [7] or in the overdamped regime [8] where elastic waves may not be excited [19].

Moreover, even though the oscillations in a_c are rather well reproduced by the Maxwell model with a Zimm correction, the agreement with the experimental values of k_c remains only qualitative (see Figs. 1(b) and 4(b)). A Rouse correction was also tried with similar results. It may be argued that the discrepancy is due to an inadequate rheological model. Indeed, standard rheometers are limited to about 15 Hz , so that rheological data had to be extrapolated to higher frequencies [7, 8].

However, we believe that the lack of agreement points

to more fundamental questions about the validity of the numerical approach. Indeed, besides lateral finite-size effects, which we ruled out at the beginning of this study, at least two important physical effects are not taken into account in the model of Ref. [9]: interfacial rheology and nonlinear bulk rheology.

First, in the numerical calculations, the air–fluid interface is modelled as purely elastic with surface tension σ , whereas in a complex fluid, σ can depend on the frequency. More importantly, the *interfacial viscoelasticity* may significantly affect the boundary conditions [20].

Second, the model of Ref. [9] relies on linear viscoelasticity. Indeed, since the instability occurs from a quiescent state, strain is expected to be “small.” Experimentally, the smallest detectable surface deformation is $\zeta \simeq 10 \mu\text{m}$. The corresponding strain rate $\dot{\gamma}$ may be estimated by $\dot{\gamma} \sim \zeta \omega k \simeq 10 \text{ s}^{-1}$ at $f = 60 \text{ Hz}$ [9]. Since the zero-shear viscosity of our fluid is $\eta_0 = G_0 \tau \simeq 7 \text{ Pa s}$, $\dot{\gamma} \simeq 10 \text{ s}^{-1}$ corresponds to a shear stress of about 70 Pa, which is far into the *nonlinear regime*. Thus, the only knowledge of the linear viscoelastic moduli G' and G'' may not be sufficient to fully account for the experiments and nonlinear effects could provide an explanation for the observed discrepancies.

More precisely, wormlike micelles are known to align under shear, leading to a shear-induced nematic state [11]. This strongly *shear-thinning* isotropic-to-nematic transition occurs for $\dot{\gamma} \simeq 0.5\text{--}50 \text{ s}^{-1}$ depending on temperature and concentration [15]. In a Faraday wave pattern, shear is localized between the crests and the troughs. Thus, above onset, aligned micelles are expected to coexist with the isotropic state and to spatially mimic the surface pattern. Finally, since the destabilized state is far from a pure shear flow, one may also wonder about the influence of nonlinear *extensional* rheology.

To conclude, the present study reveals a strong signature of elasticity on the onset of the Faraday instability in a wormlike micelle solution. This original effect results from standing elastic waves in the container height and should be very general in highly viscoelastic fluids. It shows that, as suggested earlier [8, 9], the characteristic relaxation time of a complex fluid may couple to the excitation period and/or to memory effects, leading to new temporal and spatial behaviours under vertical vibrations. Linear viscoelasticity allows for a good qualitative agreement with the model of Ref. [9] but we believe that surface rheology and/or nonlinear effects are also significant. This raises new challenges for theory and modelling of hydrodynamic instabilities in complex fluids. In particular, we point out that the presence of a shear-induced isotropic-to-nematic transition could play a major role in the pattern selection. This last remark has to be related to some very recent experimental find-

ings on vertically vibrated shear-thickening suspensions, where a rich variety of patterns such as holes and fingers was observed after a finite perturbation was applied to the surface [21]. Such an unusual behaviour was linked to the nonlinear rheological properties of the fluid. Our results on wormlike micelles provide another example of a striking effect induced by the microstructure of a complex fluid on a classical instability.

The authors wish to thank A. Colin, F. Molino, G. Ovarlez, and R. Wunenburger for fruitful discussions and the “Cellule Instrumentation” of CRPP for technical advice and design of the experiment.

-
- [1] M. Faraday, Philos. Trans. R. Soc. Lond., **52**, 319 (1831).
 - [2] T. B. Benjamin and F. Ursell, Proc. R. Soc. London A, **225**, 505 (1954).
 - [3] P. Chen and H. Viñals, Phys. Rev. Lett., **79**, 2670 (1997).
 - [4] A. Kudrolli and J. P. Gollub, Physica D, **97**, 133 (1996).
 - [5] W. S. Edwards and S. Fauve, J. Fluid Mech., **278**, 123 (1994); J. Bechhoefer, V. Ego, S. Manneville, and B. Johnson, J. Fluid Mech., **288**, 325 (1994); E. A. Cerda and C. T. Tirapegui, J. Fluid Mech., **368**, 195 (1998).
 - [6] K. Kumar and L. S. Tuckerman, J. Fluid Mech., **279**, 49 (1994).
 - [7] F. Raynal, S. Kumar, and S. Fauve, Eur. Phys. J. B, **9**, 175 (1999).
 - [8] C. Wagner, H. W. Müller, and K. Knorr, Phys. Rev. Lett., **83**, 308 (1999).
 - [9] S. Kumar, Phys. Fluids, **11**, 1970 (1999); Phys. Rev. E, **65**, 026305 (2002).
 - [10] H. W. Müller and W. Zimmermann, Europhys. Lett., **45**, 169 (1999).
 - [11] R. G. Larson, *The Structure and Rheology of Complex Fluids* (Oxford University Press, Oxford, 1999).
 - [12] R. B. Bird, R. C. Armstrong, and O. Hassager, *Dynamics of Polymeric Liquids* (Cambridge University Press, Cambridge, 1987).
 - [13] M. E. Cates, Macromolecules, **20**, 2289 (1987).
 - [14] H. Rehage and H. Hoffmann, J. Phys. Chem., **92**, 4712 (1988).
 - [15] J. F. Berret, G. Porte, and J. P. Decruppe, Phys. Rev. E, **55**, 1668 (1997).
 - [16] S. Ciliberto and J. P. Gollub, Phys. Rev. Lett., **52**, 922 (1984).
 - [17] The factor 2 in $2h$ accounts for the reflection on the container bottom while the factor 2 in $2c/f$ corresponds to the wavelength of subharmonic elastic waves (at $f/2$).
 - [18] P. Fischer and H. Rehage, Langmuir, **13**, 7012 (1997).
 - [19] J. L. Harden, H. Pleiner, and P. A. Pincus, J. Chem. Phys., **94**, 5208 (1991).
 - [20] D. A. Edwards, H. Brenner, D. T. Wasan, *Interfacial Transport Processes and Rheology* (Butterworth-Heinemann, Stonham, 1991).
 - [21] F. S. Merkt, R. D. Deegan, D. I. Goldman, E. C. Rericha, and H. L. Swinney, Phys. Rev. Lett., **92**, 184501 (2004).